

Article

Mechanochemical Preparation of Pd(II) and Pt(II) Composites with Carbonaceous Materials and Their Application in the Suzuki-Miyaura Reaction at Several Energy Inputs

Mohamed M.A. Soliman ^{1,2}, Andreia F. Peixoto ³, Ana P.C. Ribeiro ¹, Maximilian N. Kopylovich ^{1,*}, Elisabete C.B.A. Alegria ^{1,2,*} and Armando J.L. Pombeiro ¹

¹ Centro de Química Estrutural, Complexo I, Instituto Superior Técnico, Universidade de Lisboa, 1049-001 Lisboa, Portugal; mohamed.soliman@tecnico.ulisboa.pt (M.M.A.S.); apribeiro@tecnico.ulisboa.pt (A.P.C.R.); pombeiro@tecnico.ulisboa.pt (A.J.L.P.)

² Área Departamental de Engenharia Química, ISEL, Instituto Politécnico de Lisboa, 1959-007 Lisboa, Portugal

³ REQUIMTE/LAQV, Departamento de Química e Bioquímica, Faculdade de Ciências, Universidade do Porto, Rua do Campo Alegre s/n, 4169-007 Porto, Portugal; andreia.peixoto@fc.up.pt

* Correspondence: maximilian.kopylovich@tecnico.ulisboa.pt (M.N.K.); ebastos@deq.isel.ipl.pt (E.C.B.A.A.); Tel.: +351-218317163 (E.C.B.A.A.)

Academic Editors: Raquel G. Soengas and Humberto Rodríguez-Solla

Received: 28 May 2020; Accepted: 23 June 2020; Published: 26 June 2020



Abstract: Pd(II) and Pt(II) composites with activated carbon (AC), graphene oxide, and multiwalled carbon nanotubes were prepared by ball milling and used as catalysts for the Suzuki-Miyaura reaction, under several energy inputs (mechanical grinding, conventional heating, and microwave irradiation). The catalytic composites were characterized by ICP-MS, BET, XPS analyses, TEM, and SEM. The average particle size of the prepared composites was estimated to be in the range of 6–30 nm, while the loadings of Pd and Pt did not significantly affect the surface area of the AC support due to the tendency to agglomerate as observed by the TEM analysis. The Pd/AC composites exhibit high mechanochemical catalytic activity in cross-coupling of bromobenzene and phenylboronic acid with molar yields up to 80% with TON and TOF of 222 and 444 h⁻¹, respectively, achieved with Pd(4.7 wt%)-AC catalyst under the liquid assisted grinding for 0.5 h at ambient conditions, using cyclohexene as an additive.

Keywords: mechanochemical; liquid-assisted grinding; Suzuki-Miyaura reaction; cross-coupling; Palladium; Platinum; composites

1. Introduction

The Suzuki-Miyaura (SM) cross-coupling of aryl halides with aryl boronic acids to form biaryls has become an exceptionally powerful tool in organic synthesis [1–4]. The notable expansion of this reaction is based on its applicability to a wide range of substrates with various functional groups and availability of the boronic acid starting materials. Generally, this chemical transformation needs a transition metal catalyst to proceed at a synthetically useful rate, and catalysts based on Pd dominate the scene [1–4]. The homogeneous catalytic conditions were the first choice of chemists because of high activity and selectivity; however, difficulties in the catalyst recovery and product purification are obvious drawbacks even at the laboratory scale. Moreover, catalysts that are active but difficult to recycle/recover from reaction mixture are generally not favored in the chemical industry. Hence, the recovery and reusability of catalysts is critically important for a sustainable development of the SM cross-coupling processes. These issues can be overcome by e.g., the catalyst heterogenization on

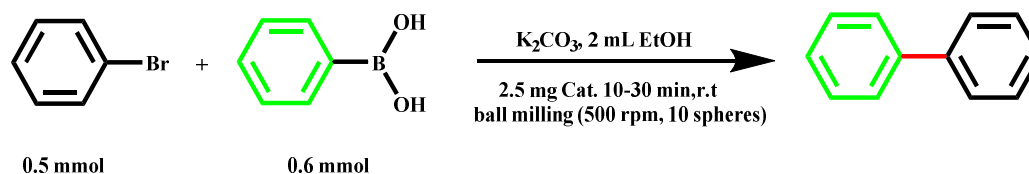
solid supports. However, in many cases the heterogenization decreases the overall catalytic efficiency, being also expensive and difficult to achieve on industrial scale. Therefore, elaboration of simple, scalable, eco-friendly and fast technics to prepare highly active and reusable dispersed catalysts for the SM reaction constitutes a significant challenge [5–7], and mechanochemical methods can eventually provide an effective solution [8–12].

The mechanochemical preparative technics involve chemical and physico-chemical transformations of substances produced by the effect of mechanical energy. These include influencing reactivity of solids by the presence of solid-state defects, interphase interactions and relaxations, which can enable time-convenient one-step syntheses of new nanomaterials with the desired properties in a reproducible way with high yields and under simple and easy operating conditions [8–12]. Due to these and other phenomena (e.g., formation of “hot spots” or mechanically stimulated phase transformations) [8], many mechanochemical processes take place under environmentally friendly and essentially waste-free conditions. Another advantage of the mechanochemical preparative technics involves their easy scaling up with the industrial milling equipment already available [8].

As it was mentioned above, Pd(II) salts or complexes are usually employed as catalytic agents for cross-couplings and related reactions. Such compounds are then reduced *in situ* to Pd(0) species which enter the catalytic cycle. The catalytic cycle involves the rate-determining activation of the aryl halide by oxidative addition, transmetalation and reductive elimination [1–7]. In each of these steps an effective charge transport from the metal nanoparticles to the π system of the aryl halides or boronic acids is important, and hence physicochemical properties of the support are relevant for the successful metal heterogenization, dispersion, charge transport, and, as result, the overall catalytic activity.

The delocalized system of π electrons of carbonaceous materials is beneficial for π - π interactions with aromatic groups of substrates and for constructing electron-enriched vacancy defects which facilitate redox processes [9,13–16]. Due to these reasons as well as their high chemical stability, mechanical resistance, large surface area, tunable electronic, and physicochemical features, the carbon-based materials are broadly used as catalysts and catalyst supports in many industrially important processes [17–21], while mechanochemical methods have been applied for their preparation and functionalization [9–12,22–24]. Moreover, the use of supported Pd may prevent its aggregation upon reduction with the respective drop in activity [1–7]. Among different carbon materials, activated carbon (AC) is the most used and studied support for Pd catalysts and in the C-C coupling chemistry due to its low price and abundance, unique chemical and mechanical properties [20,21,25–29]. Thus, carbon is a high tensile material, able to sustain the amount of energy produced in ball milling, with the advantage of not inhibiting the SM reaction. Accordingly, in this study we intend to develop this line further and to prepare new composites composed from palladium salts and activated carbon as a support and component of catalytic system. For comparative purposes, platinum salts will be also tried as the main catalytic species and graphene oxide (GO) and multiwalled carbon nanotubes (MWCNT) as supports.

From another prospective, not only the preparation of catalysts can be achieved by mechanochemical procedures, but also the catalytic reactions themselves [10,12]. The application of mechanical energy to promote C-C coupling is a hot topic nowadays, and several prominent papers have been published highlighting different aspects of this field [30–34]. The advantages of the mechanochemical treatment include decreased reaction times, simplified work-up procedures, omission or minimization of solvents and better energy balance in comparison with the conventional procedures. According to this view, in this study we intend to prepare “(metal salt)-(carbon material)” composites (where metal is Pd or Pt and carbon material is AC, GO, or MWCNT) by simple mechanochemical procedure and apply the prepared composites as catalysts in the mechanically activated SM model reaction, namely coupling of phenylboronic acid and bromobenzene as the aryl halide partner (Scheme 1). For comparative purposes, other energy inputs, such as the conventional heating in oil bath with magnetic stirring and microwave (MW) irradiation, were also studied.



Scheme 1. Suzuki-Miyaura reaction of bromobenzene and phenylboronic acid (typical reaction conditions).

2. Results and Discussion

2.1. Preparation of Pd and Pt Catalysts

Pd(II) and Pt(II) composites were prepared by ball milling using their respective $\text{Pd}(\text{CH}_3\text{COO})_2$ and K_2PtCl_4 salts as Pd and Pt sources, respectively, and commercially available AC as support (see Section 3.1., Table 1 and Electronic Supporting Material for details). The approximate theoretical metal-to-carbon ratio was 4.7 and 8.5 wt%, while the actual metal content was determined by Inductively Coupled Plasma-Mass Spectroscopy (ICP-MS, Table 2). The prepared catalysts will hereinafter be denoted as AC-Pd1 and AC-Pt1 for the theoretical metal content of ca. 4.7 wt%, and AC-Pd2 and AC-Pt2 for the respective contents of ca. 8.5 wt%. For comparative purposes, palladium composites with GO and MWCNT were similarly prepared by grinding in ball mill. As it was indicated above, the use of the carbon-based material aims to improve the catalyst activity and stability in the reaction medium, allowing its recovery and reuse [2–7,17–21,25–29].

Table 1. Denotation of the prepared composites.

Support (100 mg)	Metal Precursor	Pd(OAc) ₂		K ₂ PtCl ₄	
		11 mg	22 mg	11 mg	22 mg
AC		AC-Pd1	AC-Pd2	AC-Pt1	AC-Pt2
MWCNTs		CNT-Pd1	CNT-Pd2	CNT-Pt1	CNT-Pt2
GO		GO-Pd2			

Table 2. Composition of the Pd/AC and Pt/AC composites.

Sample	Pd(wt%)		Pt(wt%)	
	Theoretical	Found (ICP-MS)	Theoretical	Found (ICP-MS)
AC-Pd1	4.7	4.13	-	-
AC-Pd2	8.5	7.63	-	-
AC-Pt1	-	-	4.6	4.47
AC-Pt2	-	-	8.5	7.28

2.2. Characterization of the Pd/AC and Pt/AC Composites

To define the surface morphology of the prepared composites, a set of characterization techniques [ICP-MS, Scanning Electron Microscopy (SEM) and Energy Dispersive X-ray Spectroscopy (EDX), Transmission Electron Microscopy (TEM), X-ray Photoelectron Microscopy (XPS) and Brunauer-Emmett-Teller Surface Area Analysis (BET)] has been undertaken.

ICP-MS analysis of the supported Pd and Pt catalysts was carried out to evaluate the actual loading amounts of Pd and Pt on AC. As can be seen from Table 2, the actual loading amounts of Pd and Pt on AC are 4.13 wt% (for AC-Pd1), 7.63% (for AC-Pd2), 4.47% (for AC-Pt1), and 7.28% (for AC-Pt2), respectively, giving more than 80% of the full deposition.

The performed TEM (Figure 1) and SEM (Figure 2) confirmed the presence of Pd and Pt particles supported on the AC surface. The produced dispersed materials consist of non-uniform crystallites

with tendency to agglomerate (ovals in Figure 1); this creates some difficulties to define the particle size and distribution. Nevertheless, the evaluation of the particle sizes and/or agglomerates present in the prepared materials can be performed by the digital microscopy Motic plus image software, giving average particle size around 18 nm for the AC-Pd2 dispersed nanomaterial (Figure 3).

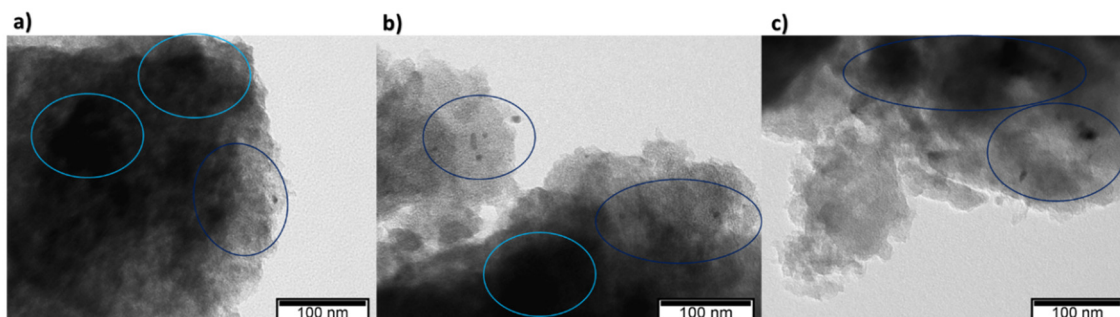


Figure 1. TEM images of AC-Pd1 (a), AC-Pd2 (b) and AC-Pt2 (c).

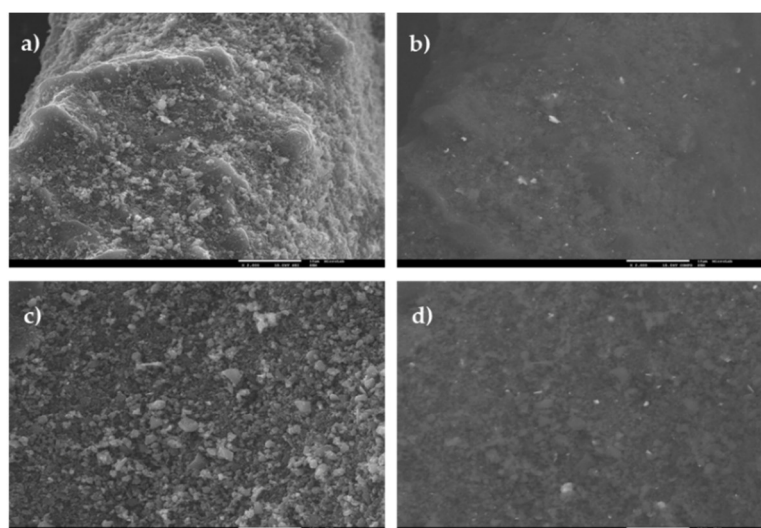


Figure 2. SEM images of AC-Pd1 (a,b), AC-Pd2 (c,d), 10 μm scale (a,c) and 2000× magnification (b,d).

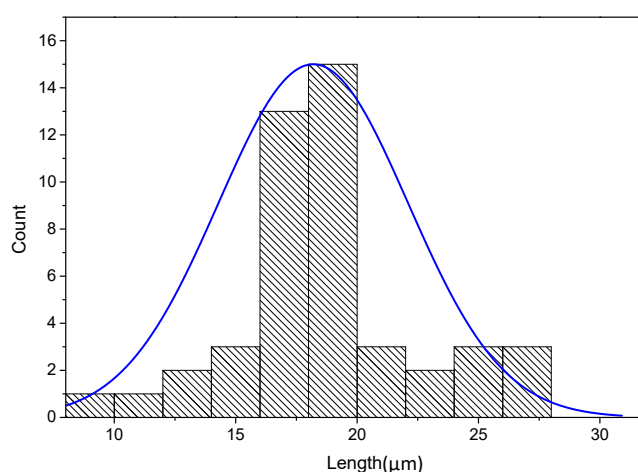


Figure 3. Particle size distribution in the AC-Pd2 sample.

The SEM images for the AC-Pd1 (Figure 2a) and AC-Pd2 (Figure 2c) composites demonstrate micro (below 1 μm) irregularities. In the back-scatter mode, the metal can be differentiated from support; elements of greater atomic mass (e.g., Pd) appear brighter in a back scattered electron

image. Both images were collected at magnification 2000 \times (Figure 2b,d for AC-Pd1 and AC-Pd2, respectively) and, as expected, the visible amount of dispersed Pd is low, what is in accordance with low Pd loadings. The EDX analysis was performed for AC-Pd1 (Figure S1a) and AC-Pd2 (Figure S1b) composites to determine the elemental composition and to confirm that Pd is the only hetero element. The EDX analysis allowed to conclude that possible contamination due to the multiple collisions between medium, reactor, and grinding balls, detected in some mechanochemical reactions [35–39], was not observed.

The qualitative and quantitative surface characterization of the Pd/AC and Pt/AC composites were also performed by XPS (Figure 4, Figures S2 and S3 and Table S1). No significant changes were observed in the high-resolution spectra of the catalysts prepared with different content of Pt or Pd precursors. High resolution Pd 3d region spectra presents a doublet corresponding to Pd 3d_{5/2} and Pd 3d_{3/2} at 337.8 and 343.1 eV suggesting the predominant presence of Pd(II) species in the surface of activated carbon (>80%) [40]. The presence of Pd(0) was not detected on the surface, although previously being identified by other authors in similar systems [41]. The small peaks observed at 340.0, 341.7 and 345.2 eV could be related to parental species from the Pd precursor [42]. The deconvolution of high-resolution spectra Pt 4f region (Figure 4) revealed two bands, each comprised of a pair of doublets: the Pt 4f_{7/2} band at low binding energy 72.2 eV and Pt 4f_{5/2} band at 75.5 eV assigned to Pt(II). The other two peaks at higher BEs 74.2 (Pt4f_{7/2}) and 77.5 eV (Pt4f_{5/2}) correspond to Pt(IV) [43]. The presence of divalent platinum in this catalyst could be due to decomposition of the platinum precursor during ball milling [44]. XPS survey analysis also revealed the presence of chlorine species on the carbon surface (Figure S2) showing an incomplete decomposition of the platinum precursor under the used experimental conditions.

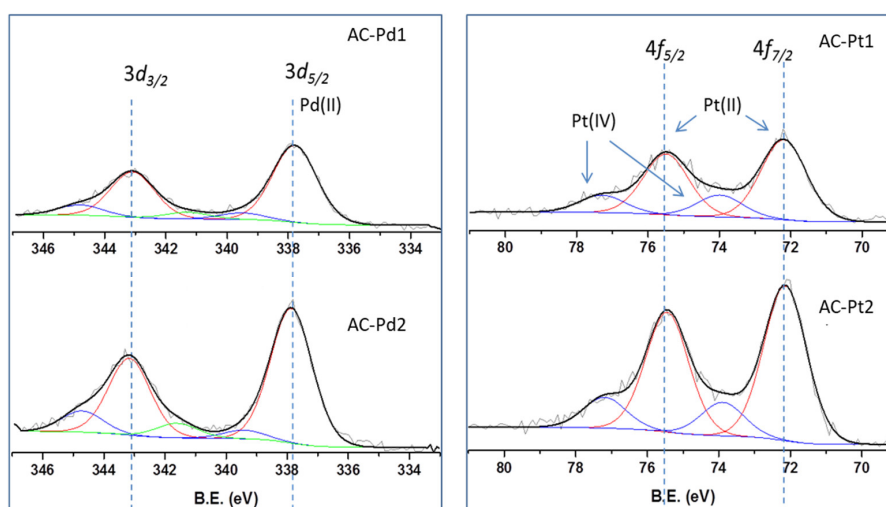


Figure 4. XPS profiles of the catalysts in the Pd 3d and Pt 4f regions.

In the carbon spectra a small peak at 290 eV was observed revealing the presence of carboxyl groups, in addition to other typical peaks including the main peak of carbon at 284.6 eV (Figure S3). Additionally, the high resolution O1s region spectra of the composites (Figure S3) give additional information about surface oxygen groups, including the peaks at ~531.5 eV attributed to C-O/C=O and M-O functional groups and different peaks at 534.2 eV for Pd/AC and at 533.3 eV for Pt/AC composites attributed to the presence of carboxylic acid and anhydride functional groups, respectively. The contribution of chemisorbed water located at 536 eV was observed in the Pd/AC samples. The ratio of total oxygen to total carbon, O/C (Table S1,) relates to the surface oxidation [45]. An increase in the oxygen content for the Pd/AC composites was observed in comparison to the pristine AC, probably as result of the carbon bonds cleavage during ball milling with the respective surface oxidation or due to a decomposition of the metal salt [41]. The XPS contents of Pd and Pt (Table S1) are lower to those

obtained by ICP (Table 1) possibly due to the tendency of the Pd and Pt nanoparticles to agglomerate, as supported also by SEM and TEM (see above).

The nitrogen adsorption-desorption isotherms for AC (Figure S7), Pd/AC and Pt/AC composites (Figure 5) were determined at $-196\text{ }^{\circ}\text{C}$. According to the IUPAC classification [46–48], a shape type (IV) isotherms and type IV (H4) hysteresis loops were observed in the relative pressure range from 0.4 to 1.0 indicating the presence of mesopores, the formation of asymmetric, slit-shaped mesopores, attributable to rapid gas evolution and open channels [46–48].

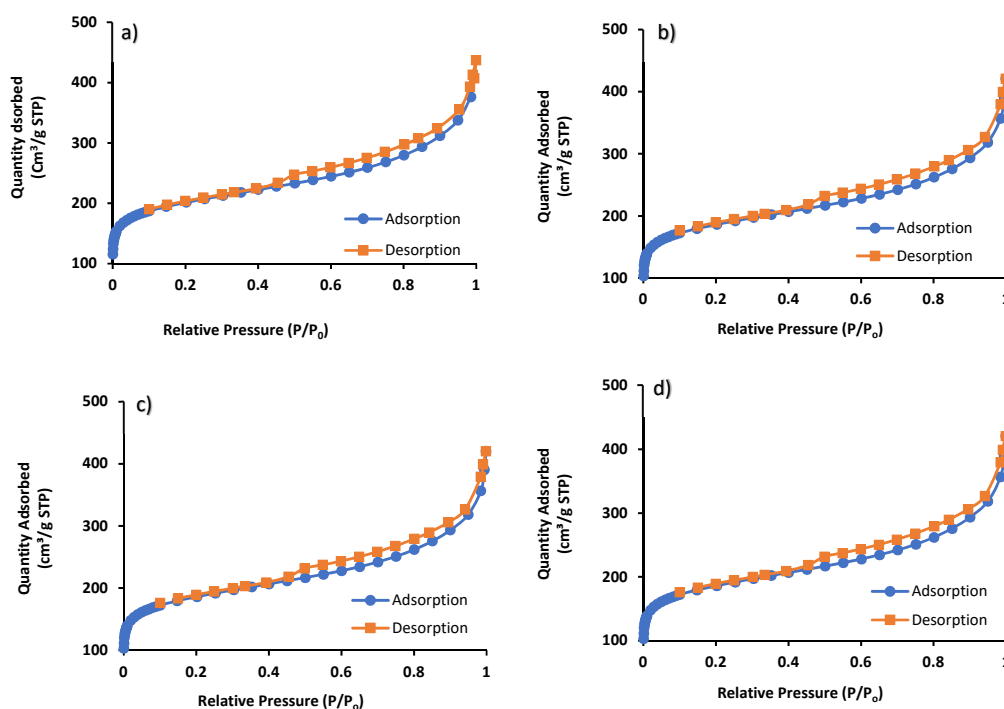


Figure 5. N_2 adsorption-desorption isotherms of synthesized AC-Pd1 (a), AC-Pd2 (b), AC-Pt1 (c), and AC-Pt2 (d) composites.

Table 3 compares the BET surface areas, pore volume and pore size of the commercial AC with those of the Pd/AC and Pt/AC supported catalysts. The surface area of the commercial AC was found to be $775\text{ m}^2/\text{g}$ with a pore volume of $0.39\text{ cm}^3/\text{g}$ and BET surface areas for the Pd/AC and Pt/AC composites arrange in the following order: AC-Pd1 ($747\text{ m}^2/\text{g}$) > AC-Pt1 ($722\text{ m}^2/\text{g}$) > AC-Pd2 ($648\text{ m}^2/\text{g}$) > AC-Pt2 ($584\text{ m}^2/\text{g}$). The surface area together with the type and percentage of supported metal correlates with the catalytic results (see below). It should also be noted that the micropores volume of the studied materials are close to the commercial AC value of $0.4\text{ cm}^3/\text{g}$, except of the AC-Pt2 composite which exhibits a lower value of $0.35\text{ cm}^3/\text{g}$. As can be seen, no drastic changes in the textural properties of the studied samples were observed, suggesting that the differences in the adsorption capacities are mainly due to their surface properties.

Table 3. Brunauer—Emmett—Teller Surface Area Analysis (BET) characterization of Pd/AC and Pt/AC composites.

Sample	S_{BET} (m^2/g)	Pore Volume (cm^3/g)	Pore Size (nm)
AC	775	0.39	6.2
AC-Pd1	747	0.42	6.9
AC-Pd2	648	0.41	7.1
AC-Pt1	722	0.40	6.9
AC-Pt2	584	0.35	7.0

2.3. Catalytic Studies

In order to investigate the effects of various parameters on the SM reaction catalyzed by the prepared composites, a model cross-coupling of bromobenzene and phenylboronic acid has been selected. Additionally, the catalytic activity of the AC-Pd2 composite was compared with Pd catalysts supported on MWCNT, GO, and CaCO₃ (Table 4). Several reaction parameters (solvent, base, reaction time) were also evaluated to maximize the yield of the coupling reaction. The commercial salts used for the preparation of composites were also tested with the same mass (2.5 mg) giving ca. 75% yield (TON 34) for Pd(OAc)₂ catalyst vs. 49% (TON 136) for the AC-Pd2 material. As can be seen, 1.5 yield drop is well compensated by the saving in Pd content. The use of commercial K₂PtCl₄ resulted in only 3% yield, indicating the importance of the AC support in improving the catalytic activity.

Table 4. Mechanochemical Suzuki–Miyaura cross-coupling reactions of bromobenzene with phenylboronic acid ^a.

Entry	Catalyst	Solvent	Base	Time (min)	Yield (%) ^b	TON ^c	TOF (h ⁻¹) ^d	
1	AC	EtOH	K ₂ CO ₃	30	0	0	0	
2	AC-Pd1	EtOH	K ₂ CO ₃	10	27	139	835	
3		EtOH	K ₂ CO ₃	30	30	155	309	
4		-	K ₂ CO ₃	30	36	186	372	
5		EtOH	K ₂ CO ₃	10	41	114	683	
6		EtOH	K ₂ CO ₃	30	49	136	272	
7		EtOH	K ₂ CO ₃	180	69	192	64	
8 ^e		EtOH	Na ₂ CO ₃	30	31	86	172	
9 ^e		EtOH	NaF	30	2	6	12	
10 ^e		AC-Pd2	EtOH	KF	30	34	94	189
11 ^e		EtOH	Cs ₂ CO ₃	30	35	97	194	
12 ^f		DCM	K ₂ CO ₃	30	3	8	17	
13 ^f		ACN	K ₂ CO ₃	30	5	14	28	
14 ^f		DMSO	K ₂ CO ₃	30	4	11	22	
15 ^f		H ₂ O	K ₂ CO ₃	30	1.6	4	9	
16		AC-Pt1	EtOH	K ₂ CO ₃	10	26	228	1.4 × 10 ³
17	EtOH		K ₂ CO ₃	30	5	44	88	
18	AC-Pt2	EtOH	K ₂ CO ₃	10	2.5	13	81	
19		EtOH	K ₂ CO ₃	30	2.3	12	25	
20	GO-Pd2	EtOH	K ₂ CO ₃	30	53	-	-	
21	CNT-Pd1	EtOH	K ₂ CO ₃	10	37	-	-	
22	CNT-Pd1	EtOH	K ₂ CO ₃	30	29	-	-	
23	CNT-Pd2	EtOH	K ₂ CO ₃	10	32	-	-	
24	CNT-Pd2	EtOH	K ₂ CO ₃	30	50	-	-	
25	CaCO ₃ _5%Pd	EtOH	K ₂ CO ₃	30	12	-	-	
26	Pd(OAc) ₂	EtOH	K ₂ CO ₃	30	75	34	68	
27	K ₂ PtCl ₄	EtOH	K ₂ CO ₃	30	3	2.5	5	

^a Reaction conditions: 2.5 mg catalyst, 0.6 mmol PhB(OH)₂, 0.5 mmol PhBr, 1.0 mmol K₂CO₃, 2 mL EtOH; ball milling: 10 milling stainless still spheres of 10 mm diameter, 500 rpm with 5 min rotation interval. ^b NMR yield (%) based on the relative integration areas of the limiting reagent (PhBr) and the product (biphenyl). ^c TON = turnover number = number of moles of product per mol of metal content, found by ICP-MS, in the catalyst. An example of TON and TOF calculation is provided in ESM. ^d TOF = TON per hour. ^e 1.0 mmol base. ^f 2 mL solvent.

Pt catalysts are not as common as the palladium ones for the SM reactions; however, application of the AC-Pt1 catalyst resulted in 26% yield (TON of 228 and TOF of $1.4 \times 10^3 \text{ h}^{-1}$) of biphenyl after 10 min (Table 4, entry 16). However, after 30 min there was a drastic reduction in yield (Table 4, entry 17), probably due to the deactivation of the catalyst. Among the palladium-based materials, the use of the AC-Pd2 composite as a catalyst resulted in the highest yields up to 49% after 30 min and 70% after 180 min (Table 4, entries 6 and 7). The catalyst with higher metal content showed higher yield (30% for AC-Pd1 relatively to 49% for AC-Pd2 after 30 min, Table 4, entry 3); however, with some decrease in TONs (155 and 136, for AC-Pd1 and AC-Pd2, respectively, after 30 min). The nanocrystalline structure of the catalysts, the absence of contaminations and the large surface area are possible reasons for the considerable conversion exhibited by this catalyst (Figure 6).

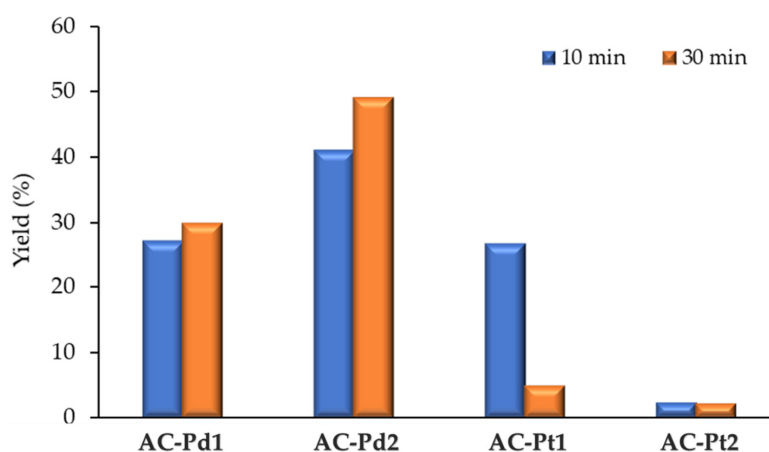


Figure 6. Cross-coupling Suzuki-Miyaura reaction of bromobenzene and phenylboronic, catalyzed by AC-Pd1, AC-Pd2, AC-Pt1, and AC-Pt2 composites. Reaction conditions: 2.5 mg catalyst, 0.6 mmol PhB(OH)₂, 0.5 mmol PhBr, 1.0 mmol K₂CO₃, 2 mL EtOH, Ball mill: 10 milling spheres, 500 rpm, rotation interval (5 min) during 10 or 30 min.

Considering the above catalyst screening, the AC-Pd2 composite was selected for the more detailed catalytic studies. Thus, several inorganic bases, namely K₂CO₃, NaF, Na₂CO₃, KF, and Cs₂CO₃, were tested for this composite, and application of potassium carbonate resulted in the highest biphenyl yield of 49% (Table 4, entry 6, Figure S8). The use of Na₂CO₃, KF and Cs₂CO₃ gave lower and similar yields in the range of 31–35% (Table 4, entries 8–10), while NaF provided the lowest product yield of 2%. Although water is considered a green solvent, its use is not beneficial as well as application of dichloromethane (DCM), acetonitrile (ACN), and dimethyl sulfoxide (DMSO), while implementation of “green” ethanol significantly improves the yield (Table 4, entries 6 and 12–15, Figure S9).

To check if replacement of the AC support by the related carbon materials would influence the catalytic results, GO and MWCNTs were used as supports (Table 4, entries 20–24). As can be seen, the AC-Pd2 catalyst (yield of 49%, Table 4, entry 6) is slightly less active than the GO-Pd2 (yield of 53%, Table 4, entry 20) and CNT-Pd2 (yield of 50%, Table 4, entry 24) analogs, under the same reaction conditions (Figure S10), while the inorganic CaCO₃ support provided a low yield of 12%, possibly due to inferior surface area.

The promoting effect of olefins [31,32], namely cyclohexene, cyclooctene and 1,5-cyclooctadiene (1,5-COD), was also explored for the so-named liquid-assisted grinding (LAG) process with the AC-Pd2 composite as a catalyst (Table 5). The presence of cyclooctene improved the yield to 59% with ethanol as a solvent (Table 5, entry 1), whereas the presence of cyclohexene and 1,5-COD dropped the yield to 19% and 21%, respectively (Table 5, entries 4 and 5). In solventless conditions, the yield increased from 59 to 80% and from 21 to 39% for the cyclooctene and 1,5-COD additives, respectively (Table 5, entries 1, 2, 5, and 6). Moreover, the addition of EtOH as an additive (0.4 μL/mg catalyst) resulted in 40% yield (Table 5, entry 7), while NaCl additive provided yield of only 28% (Table 5, entry 8).

Table 5. Effect of different additives on the Suzuki-Miyaura cross-coupling reaction of bromobenzene with phenylboronic acid by AC-Pd2 ^a.

Entry	Catalyst	Solvent	Base	Additive	Time (min)	Yield ^b	TON ^c	TOF (h ⁻¹) ^d
1	AC-Pd2	EtOH	K ₂ CO ₃	Cyclooctene	30	59	164	328
2		-		Cyclooctene	30	80	222	444
3		EtOH		Cyclooctene	180	38	106	35
4		EtOH		Cyclohexene	30	19	53	106
5		EtOH		1,5-COD	30	21	58	117
6		-		1,5-COD	30	39	108	217
7		-		EtOH	30	40	111	222
8 ^e		-		NaCl	30	27	75	150

^a Reaction conditions: 2.5 mg catalyst, 0.6 mmol PhB(OH)₂, 0.5 mmol PhBr, 1.0 mmol K₂CO₃, 2 mL EtOH; ball milling: 10 milling stainless still spheres of 10 mm diameter, 500 rpm with 5 min rotation interval. ^b NMR yield (%) based on the relative integration area of the limiting reagent (PhBr) and the product. ^c TON = turnover number = number of moles of product per mol of metal content, found by ICP-MS, in the catalyst. ^d TOF = TON per hour. ^e 0.6 g NaCl.

The effect of other than mechanical energy inputs on the catalytic output has been also studied (Table 6, Figure 7). As can be seen, in case of convectional heating (CH) for 1 h yield is higher at 35 °C in respect to 75 °C (Table 6, entry 2 vs. 5), probably due to the to the formation of Pd black with its agglomeration at higher temperatures. The CH after 30 min resulted in the complete conversion to biphenyl product, either at 75 or 35 °C, while MW irradiation has also a promoting effect since 60 min of reaction at 75 °C resulted in total conversion. However, the described above liquid assisted grinding is much more sustainable and environmentally friendly taking in consideration the energy necessary to produce and recover the used solvents.

Table 6. Effect of the other energy inputs for the solid-state Suzuki-Miyaura cross-coupling reaction of bromobenzene with phenylboronic acid by AC-Pd2 ^a.

Entry	Catalyst	Solvent	Base	Temperature (°C)	Time (min)	Yield (%) ^b	TON ^c	TOF (h ⁻¹) ^d
CH								
1	AC-Pd2	EtOH	K ₂ CO ₃	75	30	100	278	556
2					60	64	178	178
3					360	65	181	30
4				35	30	100	278	556
5					60	100	278	278
6					360	50	139	23
MW								
7	AC-Pd2	EtOH	K ₂ CO ₃	75	30	61	169	339
8					60	100	278	278
9					360	69	192	32
10				35	30	52	144	289
11					60	56	156	156
12					360	47	131	22

^a Reaction conditions: 2.5 mg catalyst, 0.6 mmol PhB(OH)₂, 0.5 mmol PhBr, 1.0 mmol K₂CO₃, 2 mL EtOH; ball milling: 10 milling stainless still spheres of 10 mm diameter, 500 rpm with 5 min rotation interval. ^b NMR yield (%) based on the relative integration area of the limiting reagent (PhBr) and the product. ^c TON = turnover number = number of moles of product per mol of metal content, found by ICP-MS, in the catalyst. ^d TOF = TON per hour. CH = conventional heating with oil bath; MW = under microwave irradiation (5–10 atm).

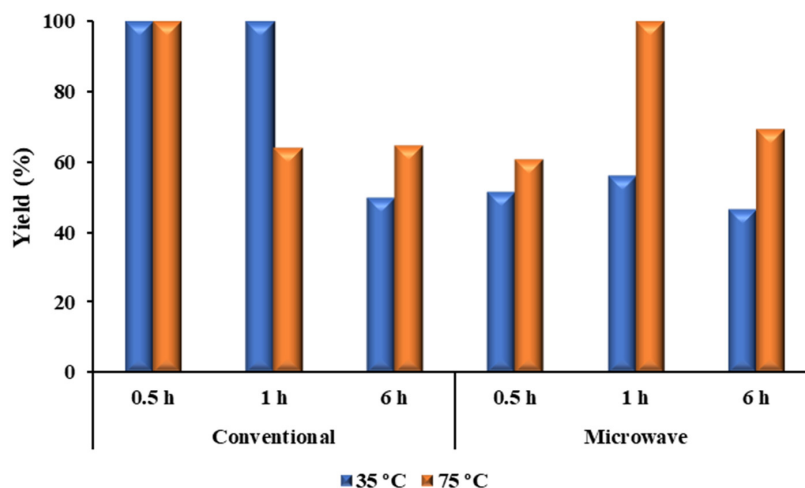


Figure 7. Conventional and microwave (MW) irradiation heating methods vs. time on the Suzuki-Miyaura (SM) reaction.

3. Materials and Methods

The activated carbon (AC, DARCO[®], −100 mesh particle size), palladium acetate Pd(OAc)₂ 47.5% Pd, ethanol, toluene, ACN, DCM, cyclohexene, 1-cyclooctene, and 1,5-cyclooctadiene were purchased from Aldrich (Sigma-Aldrich, Munich, Germany). Potassium tetrachloroplatinate(II) K₂PtCl₄ was purchased from Alfa Aesar (Kandel, Germany), bromobenzene (99%) from Panreac (Panreac, Darmstadt, Germany) and phenylboronic acid (95%) from Fluka (Fluka, Buchs, Switzerland). None of the used commercial salts is significantly sensitive to air or moisture and all the samples were handled under ambient conditions, without additional purification.

3.1. Preparation of Catalysts

The Pd and Pt-based composites were synthesized as follows: 100 mg of support (AC, GO, or MWCNT) and 11 mg or 22 mg of commercially available palladium acetate Pd(OAc)₂ or potassium tetrachloroplatinate(II) K₂PtCl₄ were added to a 250 mL stainless steel grinding bowl with 10 stainless steel balls of 10 mm diameter and milled in a Retsch PM100 planetary ball mill for 1 h at rotational speed 500 rpm, with rotational inversions every 5 min, at room temperature. All the composites were prepared in the absence of any added solvent (dry milling). All the samples were handled under ambient conditions, without additional purification of the commercial reagents.

3.2. Characterization of Catalysts

The microstructure analysis (SEM and EDX) of the catalysts was conducted with a scanning electron microscope JEOL 7001F (JEOL, Akishima, Tokyo, Japan) with Oxford light elements EDX detector and EBSD detector. The morphology of the composites was analyzed by TEM measurements and performed on a Hitachi 8100 microscope (Hitachi, Tokyo, Japan) with a ThermoNoran light elements EDX detector and digital image acquisition. ICP-MS was carried out by Microanalytical Service of the Instituto Superior Técnico. XPS was performed with a Kratos AXIS Ultra HAS (KRATOS, Manchester, UK), coupled with VISION software, at Centro de Materiais da Universidade do Porto (CEMUP), Porto, Portugal. The equipment used a monochromatic Al K α X-ray source (1486.7 eV); operation conditions: 15 kV (90 W); Fixed Analyser Transmission (FAT) mode; 40 eV (regions ROI) and 80 eV (survey) of pass energy. C1s band at 284.6 eV was used as internal standard for binding energy (BE) calibration. CASAXPS software was selected for data analysis. The BET surface areas were obtained from the N₂ adsorption isotherms collected on a Micromeritics ASAP 2060 gas sorption instrument (Hiden Isochema, Warrington, UK) at 77 K. Pre-outgassing of the samples at high vacuum at 130 °C for 24 h was undertaken to remove the physisorbed species from the surface of the examined samples.

3.3. Catalytic Studies

Typically, phenylbromide (0.5 mmol) and phenylboronic acid (0.6 mmol) as substrates, 2.5 mg composite as catalyst, potassium carbonate (1 mmol) as a base, and ethanol (2 mL) were introduced in a 250 mL stainless steel grinding jar and 10 stainless steel balls of 10 mm diameter were added. The grinding bowl was placed in the Retsch PM100 ball mill and the system was left under rotational speed 500 rpm, with rotational inversions every 5 min. At the end, 20 μ L of the reaction mixture were taken and measured amount of DMSO- d_6 was added and the sample was analyzed by ^1H NMR (for more details see Supplementary Materials). The alkene additives (1,5-COD, 1-cyclooctene, and cyclohexene) were taken in concentration 1 μ L/2.5 mg.

4. Conclusions

In this study we demonstrated a simple and sustainable way to produce Pd(II) and Pt(II) and activated carbon heterogeneous nanocomposites. The preparation involves a simple, scalable, eco-friendly and fast ball milling technique and leads to dispersed catalytic materials, highly active for the Suzuki-Miyaura mechanochemical cross-coupling of bromobenzene with phenylboronic acid. The effect of very small amounts of olefins on the reaction yield was explored and in our most promising catalytic system (in the presence of AC-Pd2 and using cyclooctene as additive), relevant yields were achieved (*ca.* 80%). Moreover, the reported results show the importance of ball milling as a promising tool, in comparison with other energy inputs, in both synthesis and catalysis, and the advantages to combine a homogeneous catalyst with a supporting material under eco-friendly conditions. The green mechanochemical method will be further explored, expanding its scope and scaling up.

Supplementary Materials: The following are available online at <http://www.mdpi.com/1420-3049/25/12/2951/s1>, Calculation of the theoretical content of metals in the composite materials, Figure S1: EDX analysis of the AC-Pd1 (a) and AC-Pd2 (b) composite materials; Figure S2: XPS survey spectra of the Pt/AC composites; Table S1. Surface atomic percentages determined by XPS for the pristine AC and within the studied Pd/AC and Pt/AC catalytic materials; Figure S3. XPS profiles of the studied Pd/AC and Pt/AC catalytic materials in C 1s and O 1s regions; Figures S4–S6: Selected ^1H NMR showing yield calculation; Figure S7: N_2 adsorption–desorption isotherms of the pristine AC; Figure S8: Effect of the different bases in the cross-coupling Suzuki–Miyaura reaction of bromobenzene and phenylboronic, catalyzed by AC-Pd2; Figure S9: Effect of the different solvents in the cross-coupling Suzuki–Miyaura reaction of bromobenzene and phenylboronic, catalyzed by AC-Pd2; Figure S10: Effect of the different supports.

Author Contributions: Conceptualization, E.C.B.A.A. and M.N.K.; Methodology, E.C.B.A.A., A.P.C.R.; Investigation, M.M.A.S. and A.F.P.; Writing-original draft preparation, M.M.A.S., E.C.B.A.A. and A.F.P.; Writing-review and editing, E.C.B.A.A., M.N.K. and A.J.L.P.; Supervision, E.C.B.A.A. and A.P.C.R.; Project administration, E.C.B.A.A.; Funding acquisition, E.C.B.A.A.; All authors have read and agreed to the published version of the manuscript.

Funding: This research was funded by MULTIFUN-Straightforward Synthesis of Multifunctional Core-Shell Composites and Their Applications, project number PTDC/QUI-QIN/29778/2017.

Acknowledgments: Financial support from the Fundação para a Ciência e a Tecnologia (FCT), Portugal (project UIDB/00100/2020 of the Centro de Química Estrutura, fellowship PD/BD/114400/2016 to M.M.A.S., contract IST-ID/219/2019 to M.N.K., UIDB/04565/2020 and PTDC/QUI-QIN/29778/2017 projects and the UID/MULTI/04046/2019 research grant), from Instituto Politécnico de Lisboa (IPL/2019/STREAM_ISEL Project) and from LAQV-REQUIMTE (UID/QUI/50006/2019). A.P.C.R. thanks Instituto Superior Técnico for the contract IST-ID/119/2018 under Decree-Law 57/2017. A.F.P. thanks FCT/MCTES the work contract (in the scope of the framework contract foreseen in the numbers 4, 5, and 6 of the article 23, of the Decree-Law 57/2016, of 29 August, changed by Law 57/2017, of 19 July) supported by national funds (OE).

Conflicts of Interest: The authors declare no conflict of interest.

References

1. Miyaura, N.; Suzuki, A. Palladium-catalyzed cross-coupling reactions of organoboron compounds. *Chem. Rev.* **1995**, *95*, 2457–2483. [[CrossRef](#)]
2. Suzuki, A. Cross-coupling reactions of organoboranes: An easy way to construct C–C bonds (Nobel lecture). *Angew. Chem. Int. Ed.* **2011**, *50*, 6723–6737. [[CrossRef](#)] [[PubMed](#)]

3. Lasri, J.; Kopylovich, M.N.; Guedes da Silva, M.F.C.; Charmier, M.A.J.; Pombeiro, A.J.L. Metal-Free and PdII-promoted [2 + 3] cycloadditions of a cyclic nitron to phthalonitriles: Syntheses of oxadiazolines as well as phthalamide–PdII and dihydropyrrolyl-iminoisindolinone–PdII complexes with high catalytic activity in Suzuki–Miyaura cross-coupling reactions. *Chem. Eur. J.* **2008**, *14*, 9312–9322. [[CrossRef](#)]
4. Lasri, J.; Guedes da Silva, M.F.C.; Kopylovich, M.N.; Mukhopadhyay, S.; Charmier, M.A.J.; Pombeiro, A.J.L. PdII-promoted [2 + 3] cycloaddition of pyrrolin N-oxide to organonitriles. Application of fused bicyclic (Δ^4 -1,2,4-oxadiazoline)-PdII complexes in the microwave-assisted Suzuki–Miyaura cross-coupling in aqueous medium. *Dalton Trans.* **2009**, *12*, 2210–2216. [[CrossRef](#)]
5. Fihri, A.; Bouhrara, M.; Nekoueishahraki, B.; Basset, J.-M.; Polshettiwar, V. Nanocatalysts for Suzuki cross-coupling reactions. *Chem. Soc. Rev.* **2011**, *40*, 5181–5203. [[CrossRef](#)] [[PubMed](#)]
6. Kohler, K.; Heidenreich, R.G.; Soomro, S.S.; Prockl, S.S. Supported palladium catalysts for Suzuki reactions: Structure-property relationships, optimized reaction protocol and control of palladium leaching. *Adv. Synth. Catal.* **2008**, *350*, 2930–2936. [[CrossRef](#)]
7. Diallo, A.K.; Ornelas, C.; Salmon, L.; Aranzaes, J.R.; Astruc, D. “Homeopathic” catalytic activity and atom-leaching mechanism in Miyaura–Suzuki reactions under ambient conditions with precise dendrimer-stabilized Pd nanoparticles. *Angew. Chem. Int. Ed.* **2007**, *46*, 8644–8648. [[CrossRef](#)] [[PubMed](#)]
8. Balaz, P.; Achimovicova, M.; Balaz, M.; Billik, P.; Cherkezova-Zheleva, Z.; Criado, J.M.; Delogu, F.; Dutkova, E.; Gaffet, E.; Gotor, F.J.; et al. Hallmarks of mechanochemistry: From nanoparticles to technology. *Chem. Soc. Rev.* **2013**, *42*, 7571–7637. [[CrossRef](#)] [[PubMed](#)]
9. Casco, M.E.; Kirchoff, S.; Leistenschneider, D.; Rauche, M.; Brunner, E.; Borchardt, L. Mechanochemical synthesis of N-doped porous carbon at room temperature. *Nanoscale* **2019**, *11*, 4712–4718. [[CrossRef](#)]
10. Alegria, E.C.B.A.; Fontolan, E.; Ribeiro, A.P.C.; Kopylovich, M.N.; Domingos, C.; Ferraria, A.M.; Bertani, R.; Botelho do Rego, A.M.; Pombeiro, A.J.L. Simple solvent-free preparation of dispersed composites and their application as catalysts in oxidation and hydrocarboxylation of cyclohexane. *Mat. Today Chem.* **2017**, *5*, 52–62. [[CrossRef](#)]
11. Fontolan, E.; Alegria, E.C.B.A.; Ribeiro, A.P.C.; Kopylovich, M.N.; Bertani, R.; Pombeiro, A.J.L. Ball milling as an effective method to prepare magnetically recoverable heterometallic catalysts for alcohol oxidation. *Inorg. Chim. Acta* **2017**, *455*, 653–658. [[CrossRef](#)]
12. Ribeiro, A.P.C.; Alegria, E.C.B.A.; Ferraria, A.M.; Botelho do Rego, A.M.; Kopylovich, M.N.; Pombeiro, A.J.L. Comparison of microwave and mechanochemical energy inputs in the catalytic oxidation of cyclohexane. *Dalton Trans.* **2018**, *47*, 8193–8198. [[CrossRef](#)] [[PubMed](#)]
13. Maharramov, A.M.; Mahmudov, K.T.; Kopylovich, M.N.; Pombeiro, A.J.L. *Non-Covalent Interactions in the Synthesis and Design of New Compounds*; John Wiley & Sons: Chichester, UK, 2016; p. 480. [[CrossRef](#)]
14. Mahmudov, K.T.; Kopylovich, M.N.; Guedes da Silva, M.F.C.; Pombeiro, A.J.L. *Noncovalent Interactions in Catalysis*; RCS Publishing: Marshfield, MO, USA, 2019; p. 653. [[CrossRef](#)]
15. Ribeiro, A.P.C.; Fontolan, E.; Alegria, E.C.B.A.; Kopylovich, M.N.; Bertani, R.; Pombeiro, A.J.L. The influence of multiwalled carbon nanotubes and graphene oxide additives on the catalytic activity of 3d metal catalysts towards 1-phenylethanol oxidation. *J. Mol. Cat. A. Chem.* **2017**, *426*, 557–563. [[CrossRef](#)]
16. Duan, X.; Sun, H.; Wang, S. Metal-free carbocatalysis in advanced oxidation reactions. *Acc. Chem. Res.* **2018**, *51*, 678–687. [[CrossRef](#)]
17. Lam, E.; Luong, J.H.T. Carbon materials as catalyst supports and catalysts in the transformation of biomass to fuels and chemicals. *ACS Catal.* **2014**, *4*, 3393–3410. [[CrossRef](#)]
18. Serp, P.; Figueiredo, J.L. *Carbon Materials for Catalysis*; John Wiley & Sons: Chichester, UK, 2009; p. 579. [[CrossRef](#)]
19. Serp, P.; Machado, B. *Nanostructured Carbon Materials for Catalysis*; RCS Publishing: Marshfield, MO, USA, 2015; p. 555. [[CrossRef](#)]
20. Rao, R.G.; Blume, R.; Hansen, T.W.; Fuentes, E.; Dreyer, K.; Moldovan, S.; Ersen, O.; Hibbitts, D.D.; Chabal, Y.J.; Schlögl, R.; et al. Interfacial charge distributions in carbon-supported palladium catalysts. *Nat. Commun.* **2017**, *8*, 340. [[CrossRef](#)]
21. Guerra, J.; Herrero, M.A. Hybrid materials based on Pd nanoparticles on carbon nanostructures for environmentally benign C–C coupling chemistry. *Nanoscale* **2010**, *2*, 1390–1400. [[CrossRef](#)]
22. Xu, C.; De, S.; Balu, A.M.; Ojedad, M.; Luque, R. Mechanochemical synthesis of advanced nanomaterials for catalytic applications. *Chem. Commun.* **2015**, *51*, 6698–6713. [[CrossRef](#)]

23. Leistenschneider, D.; Zürbes, K.; Schneidermann, C.; Grätz, S.; Oswald, S.; Wegner, K.; Klemmed, B.; Giebeler, L.; Eychmüller, A.; Borchardt, L. Mechanochemical functionalization of carbon black at room temperature. *J. Carbon Res.* **2018**, *4*, 14. [[CrossRef](#)]
24. Rak, M.J.; Friščić, T.; Moores, A. Mechanochemical synthesis of Au, Pd, Ru and Re nanoparticles with lignin as a bio-based reducing agent and stabilizing matrix. *Faraday Discuss.* **2014**, *170*, 155–167. [[CrossRef](#)]
25. Jüntgen, H. Activated carbon as catalyst support: A review of new research results. *Fuel.* **1986**, *65*, 1436–1446. [[CrossRef](#)]
26. Meryemoglu, B.; Irmak, S.; Hesenov, A.; Erbatur, O. Preparation of activated carbon supported Pt catalysts and optimization of their catalytic activities for hydrogen gas production from the hydrothermal treatment of biomass-derived compounds. *Int. J. Hydrogen Energ.* **2012**, *37*, 17844–17852. [[CrossRef](#)]
27. Arevalo-Bastante, A.; Martin-Martinez, M.; Álvarez-Montero, M.A.; Rodriguez, J.J.; Gómez-Sainero, L.M. Properties of carbon-supported precious metals catalysts under reductive treatment and their influence in the hydrodechlorination of dichloromethane. *Catalysts* **2018**, *8*, 664. [[CrossRef](#)]
28. Lin, X.; Liang, Y.; Lu, Z.; Lou, H.; Zhang, X.; Liu, S.; Zheng, B.; Liu, R.; Fu, R.; Wu, D. Mechanochemistry: A green, activation-free and top-down strategy to high-surface-area carbon materials. *ACS Sustain. Chem. Eng.* **2017**, *5*, 8535–8540. [[CrossRef](#)]
29. Monguchi, Y.; Fujita, Y.; Hashimoto, S.; Ina, M.; Takahashi, T.; Ito, R.; Nozaki, K.; Maegawa, T.; Sajiki, H. Palladium on carbon-catalyzed solvent-free and solid-phase hydrogenation and Suzuki-Miyaura reaction. *Tetrahedron* **2011**, *67*, 8628–8634. [[CrossRef](#)]
30. Hernandez, J.G.; Friscic, T. Metal-catalyzed organic reactions using mechanochemistry. *Tetrahedron Lett.* **2015**, *56*, 4253–4265. [[CrossRef](#)]
31. Jiang, Z.-J.; Li, Z.-H.; Yu, J.-B.; Su, W.-K. Liquid-assisted grinding accelerating: Suzuki–Miyaura reaction of aryl chlorides under high-speed ball-milling conditions. *J. Org. Chem.* **2016**, *81*, 10049–10055. [[CrossRef](#)]
32. Seo, T.; Ishiyama, T.; Kubota, K.; Ito, H. Solid-state Suzuki–Miyaura cross-coupling reactions: Olefin-accelerated C–C coupling using mechanochemistry. *Chem. Sci.* **2019**, *10*, 8202–8210. [[CrossRef](#)]
33. Gratz, S.; Wolfrum, B.; Borchardt, L. Mechanochemical Suzuki polycondensation—From linear to hyperbranched polyphenylenes. *Green Chem.* **2017**, *19*, 2973–2979. [[CrossRef](#)]
34. Vogt, C.G.; Gratz, S.; Lukin, S.; Halasz, I.; Etter, M.; Evans, J.D.; Borchardt, L. Direct mechanocatalysis: Palladium as milling media and catalyst in the mechanochemical Suzuki polymerization. *Angew. Chem. Int. Ed.* **2019**, *58*, 1–7. [[CrossRef](#)] [[PubMed](#)]
35. Suryanarayana, C. Mechanical alloying and milling. *Progress. Mater. Sci.* **2001**, *46*, 1–184. [[CrossRef](#)]
36. Burmeister, C.F.; Kwade, A. Process engineering with planetary ball mills. *Chem. Soc. Rev.* **2013**, *42*, 7660–7667. [[CrossRef](#)] [[PubMed](#)]
37. Vaidya, M.; Muralikrishna, G.M.; Murty, B.S. High-entropy alloys by mechanical alloying: A review. *J. Mat. Res.* **2019**, *34*, 664–686. [[CrossRef](#)]
38. Sopicka-Lizer, M. *High-Energy Ball Milling: Mechanochemical Processing of Nanopowders*; Woodhead Publishing Limited: Cambridge, UK, 2010; p. 421, ISBN 978-1-84569-531-6.
39. Gajovic, A.; Furic, K.; Tomasic, N.; Popovic, S.; Skokoc, Z.; Music, S. Mechanochemical preparation of nanocrystalline TiO₂ powders and their behavior at high temperatures. *J. Alloy. Compd.* **2005**, *398*, 188–199. [[CrossRef](#)]
40. Fan, X.; Sans, V.; Sharma, S.K.; Plucinski, P.K.; Zaikovskii, V.A.; Wilson, K.; Tennison, S.R.; Kozynchenko, A.; Lapkin, A.A. Pd/C catalysts based on synthetic carbons with bi- and tri-modal pore-size distribution: Applications in flow chemistry. *Catal. Sci. Technol.* **2016**, *6*, 2387–2395. [[CrossRef](#)]
41. Siamaki, A.R.; Lin, Y.; Woodberry, K.; Connell, J.W.; Gupton, B.F. Palladium nanoparticles supported on carbon nanotubes from solventless preparations: Versatile catalysts for ligand-free Suzuki cross coupling reactions. *J. Mater. Chem. A* **2013**, *1*, 12909–12918. [[CrossRef](#)]
42. Guerrero-Ortega, L.P.A.; Ramirez-Meneses, E.; Cabrera-Sierra, R.; Palacios-Romero, L.M.; Philippot, K.; Santiago-Ramirez, C.R.; Lartundo-Rojas, L.; Manzo-Robledo, A. Pd and Pd@PdO core-shell nanoparticles supported on Vulcan carbon XC-72R: Comparison of electroactivity for methanol electro-oxidation reaction. *J. Mater. Sci.* **2019**, *54*, 13694–13714. [[CrossRef](#)]
43. Silvestre-Albero, J.; Coloma, F.; Sepúlveda-Escribano, A.; Rodríguez-Reinoso, F. Effect of the presence of chlorine in bimetallic PtZn/CeO₂ catalysts for the vapor-phase hydrogenation of crotonaldehyde. *Appl. Catal. A-Gen.* **2006**, *304*, 159–167. [[CrossRef](#)]

44. Abdelouahab-Reddam, Z.; Mail, R.E.; Coloma, F.; Sepúlveda-Escribano, A. Platinum supported on highly-dispersed ceria on activated carbon for the total oxidation of VOCs. *Appl. Catal. A-Gen.* **2015**, *494*, 87–94. [[CrossRef](#)]
45. Figueiredo, J.L.; Pereira, M.F.R.; Freitas, M.M.A.; Orfao, J.J.M. Modification of the surface chemistry of activated carbons. *Carbon* **1999**, *37*, 1379–1389. [[CrossRef](#)]
46. Sing, K.S.W.; Everett, D.H.; Haul, R.A.W.; Moscou, L.; Pierotti, R.A.; Rouquerol, J.; Siemieniewska, T. Reporting physisorption data for gas/solid systems with special reference to the determination of surface area and porosity. *Pure. Appl. Chem.* **1985**, *57*, 603–619. [[CrossRef](#)]
47. Thommes, M.; Kaneko, K.; Neimark, A.V.; Olivier, J.P.; Reinoso, F.R.; Rouquerol, J.; Sing, K.S.W. Physisorption of gases, with special reference to the evaluation of surface area and pore size distribution (IUPAC Technical Report). *Pure. Appl. Chem.* **2015**, *87*, 1051–1069. [[CrossRef](#)]
48. Jena, H.M.; Kumar, A. Preparation and characterization of high surface area activated carbon from Fox nut (*Euryale ferox*) shell by chemical activation with H₃PO₄. *Results. Phys.* **2016**, *6*, 651–658. [[CrossRef](#)]

Sample Availability: Samples of the composites are not available from the authors.



© 2020 by the authors. Licensee MDPI, Basel, Switzerland. This article is an open access article distributed under the terms and conditions of the Creative Commons Attribution (CC BY) license (<http://creativecommons.org/licenses/by/4.0/>).